Induced pluripotent stem cell-derived motor neurons from amyotrophic lateral sclerosis (ALS) patients carrying different superoxide dismutase 1 mutations recapitulate pathological features of ALS

Wen-Chao Liu[1], Na Liu[2], Yan Wang[1], Chen Huang[1], Yan-Fang Li[1], Hao Wang[1], Xiao-Gang Li[2], Min Deng[1]

[1]Institute of Medical Innovation and Research, Peking University Third Hospital, Beijing 100191, China;
[2]Department of Neurology, Peking University Third Hospital, Beijing 100191, China.

Abstract

Background: Investigations of the pathogenic mechanisms in motor neurons (MNs) derived from amyotrophic lateral sclerosis (ALS) disease-specific induced pluripotent stem (iPS) cell lines could improve understanding of the issues affecting MNs. Therefore, in this study we explored mutant superoxide dismutase 1 (SOD1) protein expression in MNs derived from the iPS cell lines of ALS patients carrying different SOD1 mutations.

Methods: We generated induced pluripotent stem cell (iPSC) lines from two familial ALS (FALS) patients with *SOD1-V14M* and *SOD1-C111Y* mutations, and then differentiated them into MNs. We investigated levels of the SOD1 protein in iPSCs and MNs, the intracellular Ca^{2+} levels in MNs, and the lactate dehydrogenase (LDH) activity in the process of differentiation into the MNs derived from the controls and ALS patients' iPSCs.

Results: The iPSCs from the two FALS patients were capable of differentiation into MNs carrying different SOD1 mutations and differentially expressed MN markers. We detected high SOD1 protein expression and high intracellular calcium levels in both the MN and iPSCs that were derived from the two *SOD1* mutant patients. However, at no time did we observe stronger LDH activity in the patient lines compared with the control lines.

Conclusions: MNs derived from patient-specific iPSC lines can recapitulate key aspects of ALS pathogenesis, providing a cell-based disease model to further elucidate disease pathogenesis and explore gene repair coupled with cell-replacement therapy. Incremental mutant expressions of SOD1 in MNs may have disrupted MN function, either causing or contributing to the intracellular calcium disturbances, which could lead to the occurrence and development of the disease.

Keywords: Amyotrophic lateral sclerosis; Induced pluripotent stem cell; *SOD1* gene mutation; Motor neuron; SOD1 aggregation

Introduction

Amyotrophic lateral sclerosis (ALS) is a rapidly progressing, fatal, neurodegenerative disease for which no effective treatment exists. The exact ALS pathogenesis remains unclear, but recent multiple molecular events and genetic discoveries have provided important insights that implicate common pathological processes across the spectrum of ALS.[1,2] Superoxide dismutase 1 (SOD1) has been one of the most studied mutations owing to the early discovery of causative gene and the widest applications to murine models. Considerable evidence over recent years emphasizes that SOD1 mutations cause the disease via one or more toxic properties. Protein aggregation, mitochondrial dysfunction, and Ca^{2+} dysregulation were related to the toxicity of misfolded SOD1 in familial ALS (FALS).[3,4] Despite a profusion of advances promoted by the progression of pathogenic discoveries, there were no therapies that succeeded in translation of experimental observations into the clinic.[5] In part, this reflects lack of appropriate human cell-based models to demonstrate the disease mechanisms and identify promising therapeutics before long and expensive clinical trials. Human induced pluripotent stem cell (iPSC) systems with naturally occurring human pathology could complement existing murine models, potentially facilitating clinical translation and bridging this gap. Our and others' researches have previously reported that motor neurons (MNs) derived from ALS-iPSC partially elucidate the mechanisms of mutant protein-related ALS disease.[6-9]

Access this article online

Quick Response Code:

Website: www.cmj.org

DOI: 10.1097/CM9.0000000000001693

Wen-Chao Liu and Na Liu contributed equally to this work.

Correspondence to: Dr. Min Deng, Institute of Medical Innvoation and Research, Peking University Third Hospital, No. 49 Huayuan Road, Haidian District, 10091, Beijing, China
E-Mail: dengmin04@163.com

Chinese Medical Journal 2021;134(20)
Received: 28-04-2021 **Edited by:** Yan-Jie Yin and Xiu-Yuan Hao

It has recently been reported that the presence of misfolded proteins, specifically those causing protein aggregation, may disrupt several intracellular mechanisms and trigger neurotoxicity in ALS.[10] These protein aggregates exhibit intense immunoreactivity with antibodies against SOD1; they develop before the onset of the clinical disease, and in some cases, represent the earliest sign of the disease. Remarkably, as we learned using models of mutant SOD1-mediated ALS, mitochondria compromised in ALS patients is obvious from several studies that have been conducted using cellular or animal models.[11] ALS-SOD1 alters the mitochondrial protein composition and decreases the protein import into mitochondria, which then comprises part of the mitochondrial damage.[12] Moreover, mitochondrial abnormalities disturb the calcium homeostasis, as the higher intracellular calcium levels lead to possible mitochondrial Ca^{2+} overload.[13] It is important to assess whether these changes in animal models also can occur in iPSC, including the targeted types that are mainly implicated in the disease, namely MNs and astrocytes.

In the present study, we reprogrammed skin fibroblast cells into iPSCs from two FALS patients with *SOD1-V14M* and *SOD1-C111Y* mutations and from control subjects. Then these iPSCs were differentiated into MNs. Next, we investigated the levels of the SOD1 protein in both iPSCs and MNs and measured intracellular Ca^{2+} levels in the MNs. Analysis of these assays in iPSC-derived neural cells from ALS patients carrying different mutations provided insight into the convergence of the cellular and molecular mechanisms in different familial types of ALS, highlighting the importance of protein aggregation and calcium dysregulation in ALS.

Methods

Ethical approval

The study was conducted in accordance with the *Helsinki Declaration of 1975*, as revised in 2000 (5). It was approved by the Ethical Committee of Peking University Third Hospital (IRB00006761-L-2010055). Written informed consent was obtained from all participants.

Participants

The clinical data were collected and the *SOD1* gene mutations were screened from our FALS database. Then, the selected probands with *SOD1-V14M* and *SOD1-C111Y* mutations were analyzed. All ALS patients met the diagnosis of the El Escorial revised criteria.[14] Additionally, skin fibroblasts were donated from four age-matched and sex-matched healthy controls of Han Chinese descent with no previous personal or family history of neurodegenerative disease, which were used to generate iPSCs. The p.V14M mutation was observed in a 21-year-old woman, who started with weakness of the lower limb and the course of the disease lasted about 109 months. The patient carrying the p.C111Y mutation was a 70-year-old female diagnosed with ALS. She reported a 20-month history of progressive upper limb muscle weakness and the course of the disease lasted about 48 months. She died of respiratory failure.

Derivation of patient-specific fibroblast cells and mutation detection

The *SOD1-V14M* and *SOD1-C111Y* mutations were detected using polymerase chain reaction (PCR) and direct sequencing of genomic DNA. We isolated 3 mm dermal explants by a skin punch biopsy of the two FALS patients with the mutations *SOD1-V14M* and SOD1-*C111Y*. The mutation fibroblast outgrowth from the explants were passaged with trypsin, and then frozen for 1 to 2 weeks. A TIANamp Genomic DNA Kit (Qiagen, Valencia, CA, USA) was used to extract the patients' genomic DNA; genomic sequencing of the patients' DNA was performed by the BGI Genomics Co., Ltd. (Shenzhen, Guangdong, China).

Cell culture

Human fibroblast cells were cultured in fibroblast medium (FM) (Dulbecco's modified Eagle's medium [DMEM]; Gibco, Carlsbad, CA, USA), supplemented with 10% fetal bovine serum (FBS) (HyClone, Logan, UT, USA), 1 mmol/L glutamine, and 1% penicillin/streptomycin (Chemicon InternationalInc, Temecula, CA, USA). Human embryonic stem (ES) cells and iPSCs were cultured in a standard human embryonic stem cell (hESC) medium as described previously.[8,15] The human iPSC derivation medium was the same as the human iPSC culture medium, except that the concentration of fibroblast growth factor beta (bFGF) (PeproTech Inc, Cranbury, NJ, USA) was 10 ng/mL.

Retroviral production and iPS cell generation

We used a previously described protocol to generate iPSCs[16] Retroviruses (human octamer-binding transcription factor 4 (*OCT4*), SRY (sex determining region Y)-box 2 (*SOX2*), Kruppel-like factor 4 (*KLF4*), and myelocytomatosis celluar oncogene (*c-MYC*) were introduced into fibroblast cells. After 48 h of transfection, medium containing virus was collected and concentrated by centrifugation for 2 h at 22,000 r/min, 4 °C. The viral pellet was re-suspended in 1 mL FM and used to infect 5×10^4 fibroblast cells in a well of a 12-well plate. After 8 to 12 h of infection, we replaced the fresh FM with infected fibroblast cells. After 3–4 days, the cells were trypsinized, and the mitomycin C (MMC)–treated Mouse embryonic fibroblast (MEF) cells were seeded in 100 cm culture dishes. The medium we used was human iPSCs derivation medium. After 3 to 4 weeks, iPS colonies appeared, and these were mechanically passaged every 3 to 4 days.

Assessment of iPSCs pluripotency

Pluripotency of iPSCs was examined using previously protocols.[8] We confirmed pluripotency ALS-iPS and control-iPSCs by expression of pluripotency markers stage-specific embryonic antigen-4 (SSEA-4), tumor-related antigen-1-60 (TRA1-60), tumor-related antigen-1-81 (TRA1-81), Nanog, OCT3/4, SOX2 and reverse transcription PCR (RT–PCR) with three germ-layer differentiation verified by reduced expression 1 (REX1), developmental pluripotency associated protein 4 (DPPA4), Nanog, and OCT4 expression. We also performed bisulfite

treatment of genomic DNA and karyotype analysis. Finally, all clones were subcutaneously injected into the groin of severe combined immunodeficiency mice to carry out an assessment based on their ability to form teratoma *in vivo*.

Immunofluorescence staining

The cells growing on slides were fixed in 4% paraformaldehyde (PFA) for 30 min, and then permeabilized with 0.5% Triton™ X-100 for 15 min. Slides were blocked in 2.5% bovine serum albumin (Sigma-Aldrich, St. Louis, MO, USA) for 1 h and incubated in primary antibodies overnight at 4 °C, and subsequently incubated with secondary antibodies (AlexaFluor®, Invitrogen, Carlsbad, California, USA) for 1 h at room temperature. Imaging was performed using a Leica confocal microscope (Leica TCS SP8 MP, Chicago, IL). The primary antibodies included: SSEA-4 (1:500; Millipore, Billerica, MA, USA), TRA1-60 (1:500; Millipore, Billerica, MA, USA), TRA1-81 (1:500; Millipore, Billerica, MA, USA), Nanog (1:500; Cosmobio, Tokyo, Japan), OCT3/4 (1:500; Santa Cruz Biotechnology, Santa Cruz, CA, USA), SOX2 (1:500; Santa Cruz Biotechnology, Santa Cruz, CA, USA), TUJ1 (1:1000; Covance, Princeton, NJ, USA), HB9 (1:100; Developmental Studies Hybridoma Bank (DSHB), Iowa City, IA, USA), and ISL1/2 (1:200; DSHB, Iowa City, IA, USA).

MN differentiation from iPSCs

We differentiated ALS-iPS and control-iPSCs into MNs based on methods that were slightly modified from previous ones.[8,17,18] Briefly, iPSCs were placed into ultra-low adherent culture dishes and treated with embryoid body (EB) medium (DMEM/F12, 2% B27 and 1% N2; Life Technologies, Carlsbad, CA, USA), supplemented with 1% non-essential amino acid (NEAA), 200 nmol/L dorsomorphin (BioVision, Mountain View, California, USA), 10 μmol/L SB-431542 (Sigma-Aldrich, St. Louis, MO, USA), and, additionally, with 1 μmol/L retinoic acid (Sigma-Aldrich, St. Louis, MO, USA) and 50–100 ng/mL smoothened agonist (SHH; PeproTech Inc, Cranbury, NJ, USA) at a particular time. On the tenth day of EB formation, these colonies were plated onto poly-DL-ornithine and laminin (PO/LAM)-coated (Sigma-Aldrich, St. Louis, MO, USA) plates. To allow for the maturation of MNs, after 20 days of differentiation, the cultures were dissociated into single cells with papain (Sigma-Aldrich, St. Louis, MO, USA) and seeded onto PO/LAM-coated slides in Neurobasal® medium, containing 2% B27 and 1% N2, with 10 ng/mL of brain-derived neurotrophic factor (BDNF; R&D Systems, Minneapolis, MN, USA) and glial cell line-derived neurotrophic factor (GDNF; R&D Systems, Minneapolis, MN, USA).

Lactate dehydrogenase (LDH) assays for neurons

ALS and control lines could be differentiated in parallel to enable direct comparison. Over the 13 days of differentiation, the cell culture medium was collected once a week for the 13 days of differentiation from the *SOD1-V14M* (L1 and L6) and *SOD1-C111Y* (Y3 and Y8), and control lines (C3 and C12; D1). LDH activity (mU/mL) was calculated for each cell type using LDH assay kits (Abcam, Cambridge, UK). LDH activity was designed against the differentiation date, and linear models were generated by comparisons between the cell types.

Western blot for SOD1 expression in iPSCs and MNs

MN cells in the 26 to 28 days of differentiation were lysed in the radio-immunoprecipitation assay (RIPA) buffer with protease inhibitors cocktail (Roche, Basel, Switzerland). Thirty micrograms of protein was separated by 12% Tris-glycine sodium dodecyl sulphate-polyacrylamide gel electrophoresis (SDS-PAGE), and then transferred to nitrocellulose membranes and probed with anti-SOD1 (1:2000; Abcam) and anti-α-Tubulin (1:1000; Sigma-Aldrich, St. Louis, MO, USA). The densitometric analysis was performed using a CDP-Star chemiluminescent detection system (Applied Biosystems, Foster City, CA, USA).

Measurement of intracellular calcium (Ca^{2+}) in MNs

Intracellular Ca^{2+} generation was assessed using the Ca^{2+}-specific fluorescent dye Fluo 3-AM (Beyotime, Beijing, China). The MNs, plated on confocal dishes, could reach optimal confluence in the 28th day of differentiation, at which time they were washed three times with PBS and loaded with 5 μmol/L Fluo 3-AM at 37 °C for 45 min. Then they were washed with PBS, and observed under a Leica confocal microscope (Leica TCS SP8 MP, Chicago, IL). Fluo 3-AM was observed at a wavelength excitation of 488 nm.

Statistical analysis

All of the data was reported as mean ± standard deviation of the three independent experiments, and were analyzed by one-way analysis of variance (ANOVA) and Student's *t* test. Significance level was set at $P < 0.05$. Semiquantitative immunofluorescence analysis of MMP and intracellular calcium was performed with Leica Application Suite X (LAS X) software.

Results

Generation of ALS-iPSCs from fibroblast cells of FALS patients with SOD1-V14M and SOD1-C111Y mutations

We obtained dermal explants by biopsy from the two FALS patients and established their fibroblast cell lines [Figure 1A]. We recruited a total of six individuals into this study: two patients diagnosed with FALS carrying the *p.V14M* mutation and *p.C111Y* mutations in the *SOD1* gene; and four healthy individuals with no history of neurological disease (CONT). Patient-derived fibroblast cells were infected with the four Yamanaka factors—KLF4, SOX2, OCT3/4, and c-MYC.[19-21] Approximately 20 days after infection, several colonies appeared with morphology similar to that of hESCs [Figure 1B]. At least 4–6 iPSC differentiations were performed for each line, but 2–4 lines per patient among total lines were thoroughly characterized and shown to be fully reprogrammed to pluripotency. Based on this analysis, 1–2 lines from each

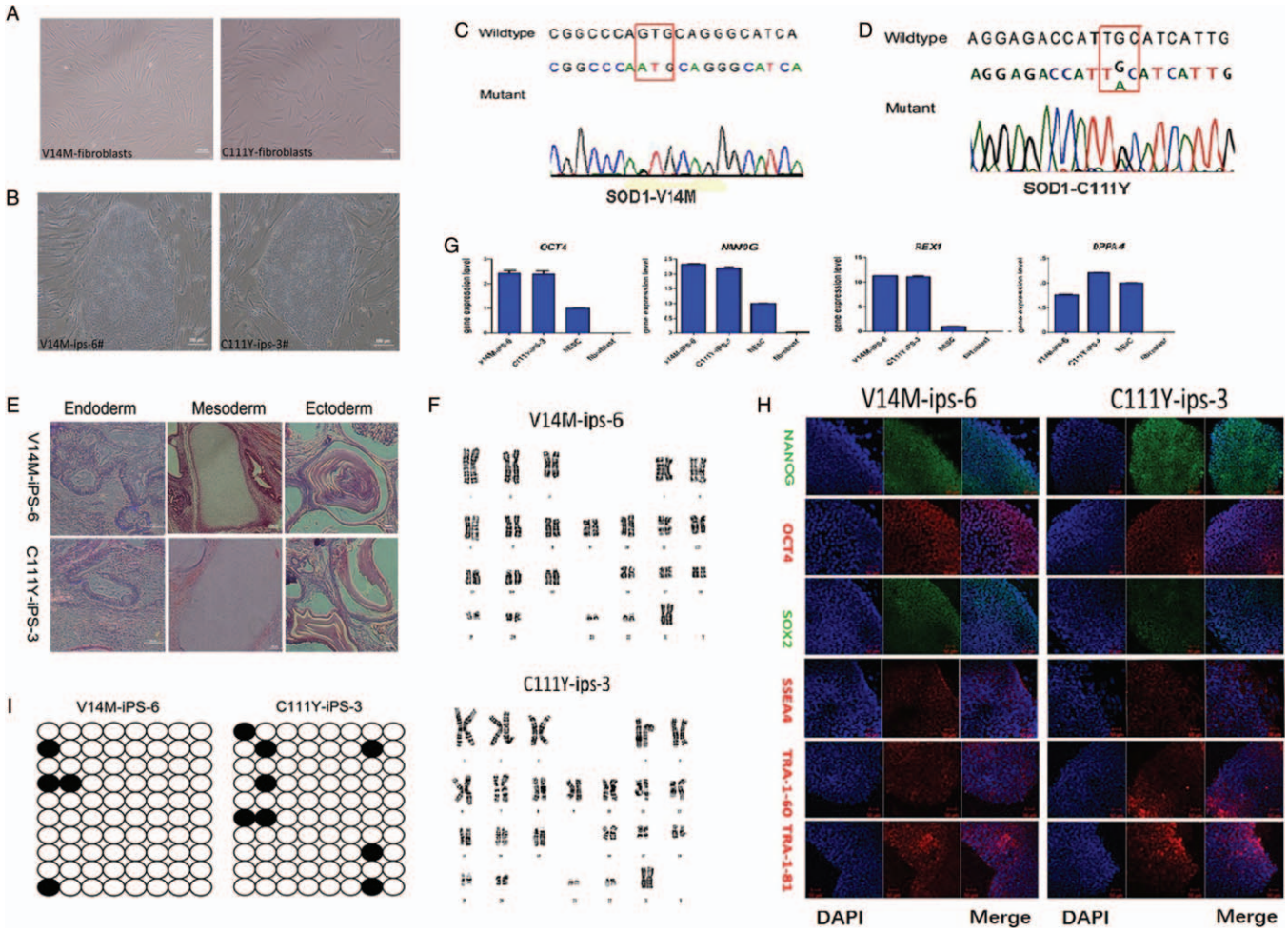

Figure 1: Generation of iPS cells from the patient's skin fibroblast carrying *SOD1-V14M* and *SOD1-C111Y* mutations, and confirmation of pluripotency. (A) Morphology of skin fibroblast cells from ALS patients with *SOD1-V14M* and *SOD1-C111Y* mutations; scale bar 100 μm. (B) Morphology of iPS cells from ALS patients with *SOD1-V14M* and *SOD1-C111Y* mutations; scale bar 100 μm. (C) There is a missense substitution of G to A in the exon 1 of the *SOD1* gene, leading to a valine to methionine substitution at residue 14 in the protein (c.43G>A). (D) A transition of G to A was detected in the exon 4 of the *SOD1* gene, resulting in a cysteine to tyrosine substitution at residue 111 in the protein (c.335G>A). (E) Histology of teratomas from the two iPS cell lines show that they contain tissue of all three germ layers, such as intestinal epithelium, cartilage, and keratinized epithelium; scale bar = 100 μm. (F) The karyotyping results of *V14M-iPS-6* and *C111Y-iPS-3* indicate that these cells are normal 46, XX human karyotype. (G) Quantitative RT-PCR results show that the endogenous pluripotent genes' expression levels of *OCT4*, *NANOG*, *DPPA4*, and *REX1* were similar to human ES cells, which is much higher than their initial fibroblast cells. (H) Both iPS cell lines express human ES cells' nuclear markers, such as OCT3/4, SOX2, and NANOG, and are also positive for the cell-surface antigens SSEA4, TRA-1-60, and TRA-1-81; scale bar = 50 μm. (I) Bisulfite genomic sequencing of NANOG promoters of these two iPS cell lines. The white and black circles represent, the unmethylated and methylated CpGs, respectively. For each iPS cell line, ten samples were sequenced, and each row indicates a repeat. SOD1: Superoxide dismutase 1; ALS: Amyotrophic lateral sclerosis; iPS: Induced pluripotent stem; RT-PCR: Reverse Transcription-Polymerase Chain Reaction; ES: Embryonic stem.

carrier were selected for further characterization: 4 lines (from four healthy individuals,) 2 from *SOD1-V14M* member, and 2 from *SOD1-C111Y* member.

Pluripotency of iPS cell lines

We identified whether the induced cells had the characteristics of typical hESCs. We focused only on the exhaustive characterization of four clones, though we originally isolated four iPSC clones from the *SOD1* mutant cells and four iPSC clones from the controls. Pluripotency results of the iPSC lines presented in two patients (*SOD1-V14M* and *SOD1-C111Y*). The genomic sequencing results illustrated that the mutation sites of the iPSCs of the two patients were *SOD1-V14M* [Figure 1C], and *SOD1-C111Y* [Figure 1D], which were identical to their parental fibroblast cells. When injected into nude mice, these induced cells developed into teratoma formation, indicating that the tissues contained different types of ectoderm, mesoderm, and endoderm tissues, including intestinal epithelium, muscle, and neural tube [Figure 1E]. The G-banding of genomic DNA showed that karyotype of these cells was normal: 46, XX human [Figure 1F]. The expression levels of undifferentiated ES cell marker genes (*DPPA4*, *NANOG*, *REX1*, and *OCT4*) in these induced cell lines were similar to those of hESCs by *RT-PCR*, but evidently lower than those in the initial fibroblasts [Figure 1G]. Moreover, immunohistochemistry displayed that several widely used hESC markers (OCT4, Nanog, TRA-1-60, SOX2, SSEA4, and TRA-1-81) were expressed in patient-specific iPSCs [Figure 1H]. Bisulfite genomic sequencing was shown to be highly unmethylated when compared to analyzed methylation status of cytosine-guanine (CpG) dinucleotides in the promoter regions of the *Nanog* gene;

this was not observed in their initial fibroblasts [Figure 1I]. In summary, this data demonstrated that fibroblasts were successfully reprogrammed into a pluripotent state and that the two SOD mutations in iPSCs did not disturb with pluripotency.

Neural differentiation of ALS patient-derived iPSc

To verify whether there were obvious defects in the MNs generated from the two SOD1-iPSCs, we induced MN differentiation based on a previously published method with slight modifications.[8,17] Schematic protocol for the differentiation process is illustrated in Figure 2A. Floating cultivation of EBs was detected at day 6 [Figure 2B]. After 14 days of differentiation, we found neural, progenitor-like outgrowths from the plated EBs that interacted with each other [Figure 2B]. After 28 days of differentiation, MN-like cells were found in our cultures [Figure 2B]. Immunofluorescence co-staining was performed with neuron-specific class III-b-tubulin (TUJ1), HB9, and ISL1 to confirm whether that these cells were MNs. As a result, we found that the HB9-positive cells or ISL1-positive cells co-expressed the MN-specific markers TUJ1 [Figure 2C]. Interestingly, we found no significant difference in the number of ISL, TUJ1, and HB9 between patients and controls at day 28 (Figure 2D, TUJ1/HB9: $F = 0.7390$, $P > 0.05$; HB9/ 4',6-diamidino-2-phenylindole(DAPI): $F = 0.2740$, $P > 0.05$; Figure 2E, TUJ1/ISL1 $F = 0.0847$, $P > 0.05$; ISL1/ADPI: $F = 0.4593$, $P > 0.05$; Tukey's Multiple Comparison Test, one-way ANOVA). Thus, our results confirmed the similar ability of control and ALS iPSC to give rise to MNs.

Comparable viability of neurons derived from all iPSC lines

Having established the equivalent MN cultures from both ALS-iPSC lines and the control-iPSC, we investigated if there were any differences in cell viability between the neurons derived from those from the ALS-iPSCs and the control group. We made quantitative analyses of cell viability using the cellular release of LDH. Analysis of LDH activity in *SOD1-V14M* and *SOD1-C111Y* showed no greater LDH activity in the patients at any time during the 4 weeks in culture, compared with the control lines (Figure 3A; $P < 0.05$); however, the level of LDH activity in the differentiation process decreased [Figure 3A].

SOD1 protein levels with specific mutation in iPSCs and MNs

A cytoplasmic SOD1 mutant inclusions are a likely key pathological feature of ALS.[22] Thus, we next detected SOD1 protein levels by Western blotting, and discovered that the MNs and iPSCs in *SOD1-V14M* and *SOD1-C111Y* exhibited higher SOD1 levels than the levels of the controls (Figure 3B; Figure 3C: $F = 28.5100$, $P < 0.05$, Tukey's Multiple Comparison Test, one-way ANOVA; Figure 3D: $F = 50.2700$, $P < 0.05$, Tukey's Multiple Comparison Test, one-way ANOVA).

Intracellular Ca^{2+} levels in MNs with specific mutation

It remains unclear whether the different SOD1 mutant that was linked to mitochondrial dysfunction occurs in ALS pathophysiology. Mitochondrial dysfunction is associated with calcium dysregulation.[23] In the present study, as expected, ALS-MNs had significantly higher intracellular Ca^{2+} than the controls' (Figure 3E and F: $F = 215.4000$, $P < 0.05$, Tukey's Multiple Comparison Test, one-way ANOVA). Similarly, there was a difference in the *SOD1-V14M* and *SOD1-C111Y* mutations (Figure 3F; $P < 0.05$, Tukey's Multiple Comparison Test). Taken together, we found that mitochondrial dysfunction occurs in ALS patients with the different SOD1 mutant.

Discussion

Disease models are indispensable tools for elucidating disease mechanisms which can be used to identify novel therapeutics. As limited availability of primary patient cells in small quantities, transgenic animals or transformed cell lines were usually used. Unlike conventional models, iPSCs, derived from patients with genetic mutation naturally occurring in ALS patients, are likely to manifest disease phenotypes. Whereas, there are still some problems that hinder utilization of disease models using human ES cells, particularly owing to the genetic variation among patients and the heterogeneity of target neural types for epigenetic changes. To overcome genetic variation, we generated iPSCs from ALS patients with different mutations (*SOD1-V14M* and *SOD1-C111Y*), and then differentiated these iPSCs into MNs damaged in ALS. Further, we used a patient-specific iPSC model to recapitulate the pathology of SOD1-related disorders. Similar to other iPSC studies of carrying ALS-associated mutations, none of the two different SOD1 mutations affected the differentiation of ALS-iPSCs into MNs.

Various ALS-SOD1 mouse models and FALS patients have been analyzed previously.[24-26] In our study, MNs and iPSCs from patients carrying different mutations exhibited much higher SOD1 protein levels compared to the controls'. However, we did detect cytoplasmic mis-localization and the formation of FUS-immuno-positive inclusions aggregates in the MNs differentiated from ALS patient-specific iPSCs carrying the *FUS-P525L* mutation.[8] This result is contrary to previous reports, in which the SOD1 level is not increased in human ALS MNs, alike to the unchanged SOD1 level in spinal cord homogenates from ALS patients.[27] However, the exact mechanism of ALS patients with lower SOD1 level in human ALS MNs compared to previously reported in mouse models presents similar phenotypes that is still not known.

Next, we performed metabolic assays to monitor the intracellular Ca^{2+}. As expected, the MNs had significant changes in intracellular Ca^{2+} assays than the controls'. Mitochondria plays a crucial role in Ca^{2+} signaling in MNs.[28] Additionally, SOD1 proteins can disrupt fundamental Ca^{2+} signaling pathways in MNs, and Ca^{2+} itself can directly or indirectly impact many ALS-related proteins and cellular processes.[4] Mitochondrial dysfunction and damage occur in both SALS and FALS. Yet, it is still unknown whether there is a causal relationship between mitochondrial alteration and mutant proteins for recently discovered ALS-linked mutations such as *FUS*,

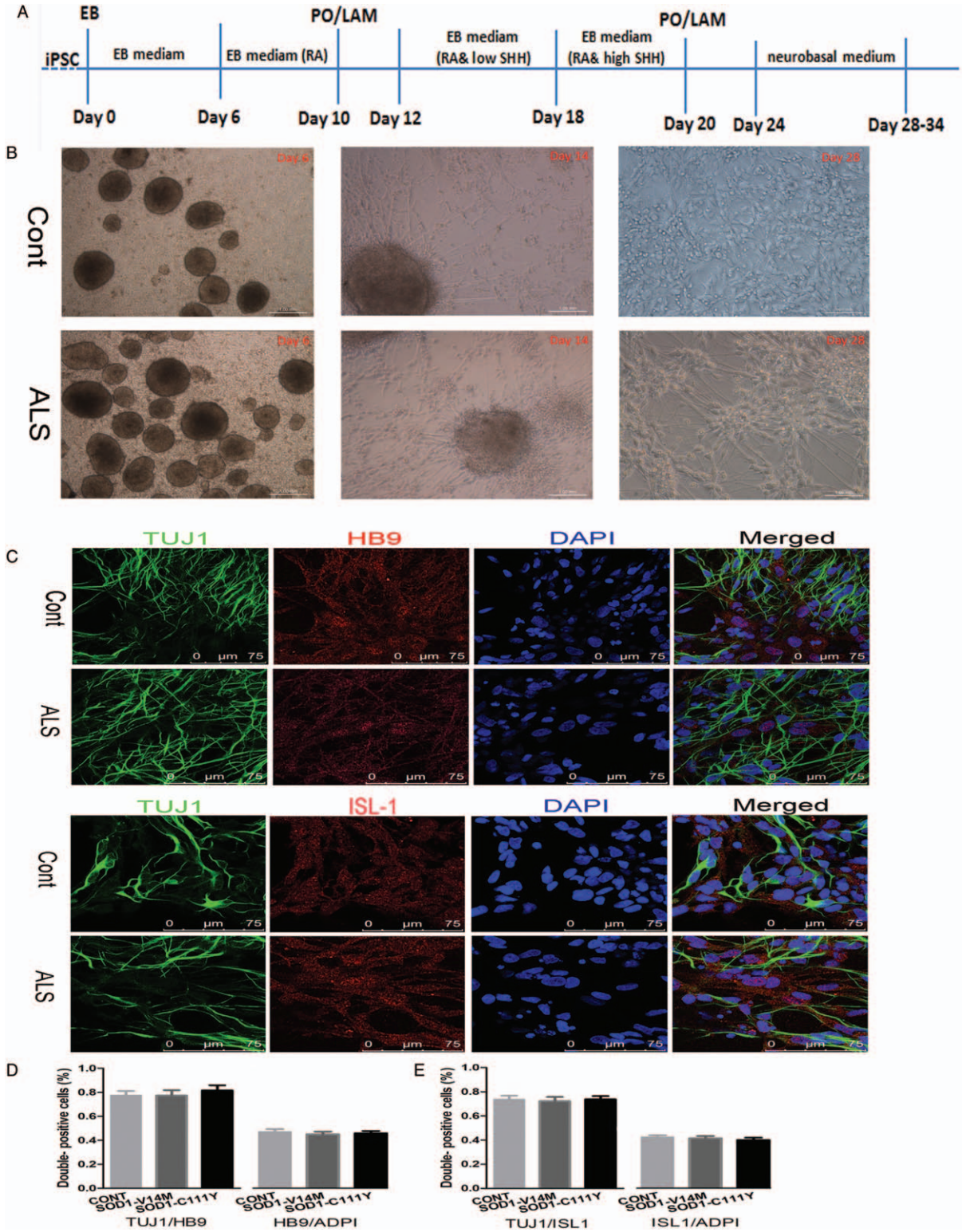

Figure 2: Differentiation of human iPS cells into motor neurons. (A) Overview of human iPS cell differentiation into MNs. EB medium (DMEM/F12, containing 2% B27 and 1% N2, supplemented with 1% NEAA, 200 nmol/L dorsomorphin, 10 μmol/L SB-431542), RA retinoic acid, low and high SHH 50-100 ng/mL sonic hedgehog, PO/LAM, neurobasal medium (2% B27 and 1% N2, with 10 ng/mL BDNF and GDNF). (B) The representative image of morphology of EBs at day 6, neural progenitors at day 14, and motor neuron-like cells at day 28 of controls (control cell line:cell line C3) and ALS patients (SOD1-V14M: cell line: L6); scale bar 1.00 mm. (C) Immunostaining of control and patient-specific MN cultures; motor neurons co-express TUJ1/HB9 and TUJ1/ISL1, nuclei are counterstained with DAPI, shown in blue; scale bar = 50 μm. (D) Quantitative analyses of cells co-express positive for TUJ1/HB9. Bars represent average with SEM as error bars. Data for CONT is the average of 4 iPSC lines, for ALS from 4 iPSC lines. No significant differences were found in the ability of iPSC to generate neurons after 28 days of differentiation. (E) Quantitative analyses of cells co-express positive for TUJ1/ISL1. iPS: Induced pluripotent stem; MNs: Mechanisms in motor neurons; EB: Embryoid body; BDNF: Brain-derived neurotrophic factor; GDNF: Glial cell line-derived neurotrophic factor; SEM: Standard error of mean; CONT: Healthy individuals with no history of neurological disease; PO/LAM: Poly-DL-ornithine and laminin; NEAA: Non-essential amino acid; DAPI: 4′, 6-diamidino-2-phenylindole.

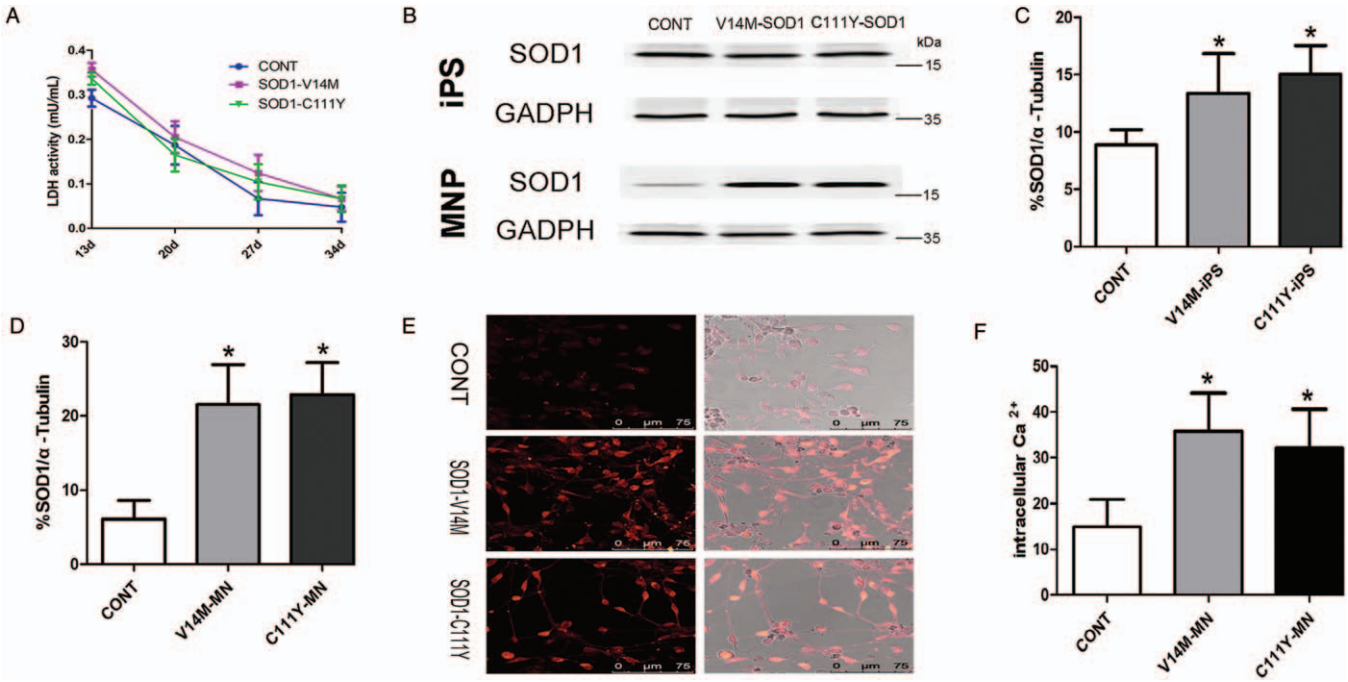

Figure 3: Comparison of cell viability, levels of SOD1 protein and intracellular Ca2+ levels in controls and ALS patients. (A) LDH activity plotted for both control and patient iPSC-derived cultures between day 13 and 34 (SOD1-V14M, SOD1-C111Y and control lines; data is plotted as mean ± SD). Data was the mean of the three independent experiments. (B) Representative blots of SOD1 protein levels, as assessed by Western blot analysis in iPSCs and MNs. (C) The proportion of the SOD1 protein in iPSCs ($F = 28.51$, $^{*}P < 0.05$, Tukey's Multiple Comparison Test, one-way ANOVA). (D) The proportion of the SOD1 protein in MNs; ($F = 50.27$, $^{*}P < 0.05$, Tukey's Multiple Comparison Test, one-way ANOVA). (E) ALS increased intracellular Ca^{2+} levels in MNs compared to controls in fluorescent microscopy. (F) Fluorescent microscopy analysis of the production of intracellular Ca2+ change in ALS-MNs ($F = 215.4$, $^{*}P < 0.05$, Tukey's Multiple Comparison Test, one-way ANOVA (Number: CONT = 41, SOD1-V14M = 24, SOD1-C111Y = 32). SOD1: superoxide dismutase 1; LDH: lactate dehydrogenase; SD: Standard deviation; iPSC: induced pluripotent stem cell; ANOVA: Analysis of Variance; ALS: amyotrophic lateral sclerosis.

TDP-43, and chromosome 9 open reading frame 72 (*C9ORF72*); however, this has been studied in great detail with mutations. IPSC-derived MNs exhibit disturbances in mitochondrial morphology and motility, which is dependent on the presence of the SOD1A4V mutation.[29] Mutant SOD1 aggregates interacted with Bcl-2 in spinal cord mitochondria, affecting mitochondrial function, and ultimately led to cell death.[30] Cytoplasmic aggregates of SOD1 might inhibit conductance of voltage-dependent anion channel (*VDAC1*), decreasing the supply of ADP to the mitochondria for ATP synthesis, which induces mitochondrial dysfunction.[11,31] Moreover, the mitochondria in both mouse and human spinal cords with SOD1 mutations increased susceptibility to oxidative stress and structural damage, which ultimately led to the release of cytochrome c.[11,32] The heterogeneity of genetic and phenotype, as well as the failure to identification of a candidate therapeutic reinforce the opinion that ALS is a multifactorial neurodegenerative disease. Also, the analysis needs to contain information as to whether the multiple manifestations of toxicity of mutant proteins in SOD1 iPSC-derived neurons are linked to a particular mutation, since in our study multiple lines and patients need to be analyzed.

In summary, we obtained iPSC lines from two FALS patients with *SOD1-V14M* and *SOD1-C111Y* mutations. These ALS-iPSC lines are pluripotent and capable of differentiation into MNs. Increased SOD1 protein, and calcium dysregulation, were observed in SOD1 iPSC-derived neurons. Multiple manifestations of the toxicity of mutant proteins in SOD1 iPSC-derived neurons could facilitate the identification of useful combination therapies for further testing.

Acknowledgements

The authors acknowledge all the individuals with ALS, their families, and healthy control subjects whose contributions made this work possible. We also thank Professors ShaoRong Gao and JiaYu Chen (School of Life Science and Technology, Tongji University, Shanghai 200092, China) for giving help on the experiments.

Funding

The study was supported by grants from National Natural Science Foundation of China (No. 31670987) and the Beijing Science Foundation (No. 7192223).

Conflicts of interest

None.

References

1. Renton AE, Chio A, Traynor BJ. State of play in amyotrophic lateral sclerosis genetics. Nat Neurosci 2014;17:17–23. doi: 10.1038/nn.3584.
2. Deng M, Wei L, Zuo X, Tian Y, Xie F, Hu P, *et al*. Genome-wide association analyses in Han Chinese identify two new susceptibility loci for amyotrophic lateral sclerosis. Nat Genet 2013;45:697–700. doi: 10.1038/ng.2627.

3. Hayashi Y, Homma K, Ichijo H. SOD1 in neurotoxicity and its controversial roles in SOD1 mutation-negative ALS. Adv Biol Regul 2016;60:95–104. doi: 10.1016/j.jbior.2015.10.006.
4. Leal SS, Gomes CM. Calcium dysregulation links ALS defective proteins and motor neuron selective vulnerability. Front Cell Neurosci 2015;9:225. doi: 10.3389/fncel.2015.00225.
5. Musaro A. Understanding ALS: new therapeutic approaches. FEBS J 2013;280:4315–4322. doi: 10.1111/Febs.12087.
6. Bilican B, Serio A, Barmada SJ, Nishimura AL, Sullivan GJ, Carrasco M, *et al*. Mutant induced pluripotent stem cell lines recapitulate aspects of TDP-43 proteinopathies and reveal cell-specific vulnerability. Proc Natl Acad Sci U S A 2012;109:5803–5808. doi: 10.1073/pnas.1202922109.
7. Almeida S, Gascon E, Tran H, Chou HJ, Gendron TF, Degroot S, *et al*. Modeling key pathological features of frontotemporal dementia with C9ORF72 repeat expansion in iPSC-derived human neurons. Acta Neuropathol 2013;126:385–399. doi: 10.1007/s00401-013-1149-y.
8. Liu X, Chen J, Liu W, Li X, Chen Q, Liu T, *et al*. The fused in sarcoma protein forms cytoplasmic aggregates in motor neurons derived from integration-free induced pluripotent stem cells generated from a patient with familial amyotrophic lateral sclerosis carrying the FUS-P525L mutation. Neurogenetics 2015;16:223–231. doi: 10.1007/s10048-015-0448-y.
9. Wainger BJ, Kiskinis E, Mellin C, Wiskow O, Han SSW, Sandoe J, *et al*. Intrinsic membrane hyperexcitability of amyotrophic lateral sclerosis patient-derived motor neurons. Cell Rep 2014;7:1–11. doi: 10.1016/j.celrep.2014.03.019.
10. Bunton-Stasyshyn RKA, Saccon RA, Fratta P, Fisher EM. SOD1 function and its implications for amyotrophic lateral sclerosis pathology: new and renascent themes. Neuroscientist 2015;21:519–529. doi: 1073858414561795.
11. Pickles S, Destroismaisons L, Peyrard SL, Cadot S, Rouleau GA, Brown RH Jr, *et al*. Mitochondrial damage revealed by immunoselection for ALS-linked misfolded SOD1. Hum Mol Genet 2013;22:3947–3959. doi: 10.1093/hmg/ddt249.
12. Li Q, Velde CV, Israelson A, Xie J, Bailey AO, Dong MQ, *et al*. ALS-linked mutant superoxide dismutase 1 (SOD1) alters mitochondrial protein composition and decreases protein import. Proc Natl Acad Sci U S A 2010;107:21146–21151. doi: 10.1073/pnas.1014862107.
13. Guatteo E, Carunchio I, Pieri M, Albo F, Canu N, Mercuri NB, *et al*. Altered calcium homeostasis in motor neurons following AMPA receptor but not voltage-dependent calcium channels' activation in a genetic model of amyotrophic lateral sclerosis. Neurobiol Dis 2007;28:90–100. doi: 10.1016/j.nbd.2007.07.002.
14. Brooks BR. El-Escorial world federation of neurology criteria for the diagnosis of amyotrophic-lateral-sclerosis. J Neurol Sci 1994;124:96–107. doi: 10.1016/0022-510x(94)90191-0.
15. Gao Y, Chen J, Li K, Wu T, Huang B, Liu W, *et al*. Replacement of Oct4 by Tet1 during iPSC induction reveals an important role of DNA methylation and hydroxymethylation in reprogramming. Cell Stem Cell 2013;12:453–469. doi: 10.1016/j.stem.2013.02.005.
16. Takahashi K, Okita K, Nakagawa M, Yamanaka S. Induction of pluripotent stem cells from fibroblast cultures. Nat Protoc 2007;2:3081–3089. doi: 10.1038/nprot.2007.418.
17. Ding Q, Lee YK, Schaefer EA, Peters DT, Veres A, Kim K, *et al*. A TALEN genome-editing system for generating human stem cell-based disease models. Cell Stem Cell 2013;12:238–251. doi: 10.1016/j.stem.2012.11.011.
18. Yang YM, Gupta SK, Kim KJ, Powers BE, Cerqueira A, Wainger BJ, *et al*. A small molecule screen in stem-cell-derived motor neurons identifies a kinase inhibitor as a candidate therapeutic for ALS. Cell Stem Cell 2013;12:713–726. doi: 10.1016/j.stem.2013.04.003.
19. Kang L, Wang J, Zhang Y, Kou Z, Gao S. iPS cells can support full-term development of tetraploid blastocyst-complemented embryos. Cell Stem Cell 2009;5:135–138. doi: 10.1016/j.stem.2009.07.001.
20. Jiao J, Yang Y, Shi Y, Chen J, Gao R, Fan Y, *et al*. Modeling Dravet syndrome using induced pluripotent stem cells (iPSCs) and directly converted neurons. Hum Mol Genet 2013;22:4241–4252. doi: 10.1093/Hmg/Ddt275.
21. Le R, Kou Z, Jiang Y, Li M, Huang B, Liu W, *et al*. Enhanced telomere rejuvenation in pluripotent cells reprogrammed via nuclear transfer relative to induced pluripotent stem cells. Cell Stem Cell 2014;14:27–39. doi: 10.1016/j.stem.2013.11.005.
22. Prudencio M, Durazo A, Whitelegge JP, Borchelt DR. Modulation of mutant superoxide dismutase 1 aggregation by co-expression of wild-type enzyme. J Neurochem 2009;108:1009–1018. doi: 10.1111/j.1471-4159.2008.05839.
23. Turner MR, Hardiman O, Benatar M, Brooks BR, Chio A, de Carvalho M, *et al*. Controversies and priorities in amyotrophic lateral sclerosis. Lancet Neurol 2013;12:310–322. doi: 10.1016/S1474-4422(13)70036-X.
24. Karch CM, Prudencio M, Winkler DD, Hart PJ, Borchelt DR. Role of mutant SOD1 disulfide oxidation and aggregation in the pathogenesis of familial ALS. Proc Natl Acad Sci U S A 2009;106:7774–7779. doi: 10.1073/pnas.0902505106.
25. Wang J, Slunt H, Gonzales V, Fromholt D, Coonfield M, Copeland NG, *et al*. Copper-binding-site-null SOD1 causes ALS in transgenic mice: aggregates of non-native SOD1 delineate a common feature. Hum Mol Genet 2003;12:2753–2764. doi: 10.1093/Hmg/Ddg312.
26. Prudencio M, Hart PJ, Borchelt DR, Andersen PM. Variation in aggregation propensities among ALS-associated variants of SOD1: correlation to human disease. Hum Mol Genet 2009;18:3217–3226. doi: 10.1093/Hmg/Ddp260.
27. Chen H, Qian K, Du Z, Cao J, Petersen A, Liu H, *et al*. Modeling ALS with iPSCs reveals that mutant SOD1 misregulates neurofilament balance in motor neurons. Cell Stem Cell 2014;14:796–809. doi: 10.1016/j.stem.2014.02.004.
28. Jahn K, Grosskreutz J, Haastert K, Ziegler E, Schlesinger F, Grothe C, *et al*. Temporospatial coupling of networked synaptic activation of AMPA-type glutamate receptor channels and calcium transients in cultured motoneurons. Neuroscience 2006;142:1019–1029. doi: 10.1016/j.neuroscience.2006.07.034.
29. Kiskinis E, Sandoe J, Williams LA, Boulting GL, Moccia R, Wainger BJ, *et al*. Pathways disrupted in human ALS motor neurons identified through genetic correction of mutant SOD1. Cell Stem Cell 2014;14:781–795. doi: 10.1016/j.stem.2014.03.004.
30. Pasinelli P, Belford ME, Lennon N, Bacskai BJ, Hyman BT, Trotti D, *et al*. Amyotrophic lateral sclerosis-associated SOD1 mutant proteins bind and aggregate with Bcl-2 in spinal cord mitochondria. Neuron 2004;43:19–30. doi: 10.1016/j.neuron.2004.06.021.
31. Israelson A, Arbel N, Da Cruz S, Ilieva H, Yamanaka K, Shoshan-Barmatz V, *et al*. Misfolded mutant SOD1 directly inhibits VDAC1 conductance in a mouse model of inherited ALS. Neuron 2010;67:575–587. doi: 10.1016/j.neuron.2010.07.019.
32. Pedrini S, Sau D, Guareschi S, Bogush M, Brown RH Jr, Naniche N, *et al*. ALS-linked mutant SOD1 damages mitochondria by promoting conformational changes in Bcl-2. Hum Mol Genet 2010;19:2974–2986. doi: 10.1093/hmg/ddq202.

How to cite this article: Liu WC, Liu N, Wang Y, Huang C, Li YF, Wang H, Li XG, Deng M. Induced pluripotent stem cell-derived motor neurons from amyotrophic lateral sclerosis (ALS) patients carrying different superoxide dismutase 1 mutations recapitulate pathological features of ALS. Chin Med J 2021;134:2457–2464. doi: 10.1097/CM9.0000000000001693